

This is the accepted manuscript made available via CHORUS. The article has been published as:

# Probing Anisotropic Superfluidity in Atomic Fermi Gases with Rashba Spin-Orbit Coupling

Hui Hu, Lei Jiang, Xia-Ji Liu, and Han Pu

Phys. Rev. Lett. **107**, 195304 — Published 4 November 2011

DOI: [10.1103/PhysRevLett.107.195304](https://doi.org/10.1103/PhysRevLett.107.195304)

# Probing anisotropic superfluidity in atomic Fermi gases with Rashba spin-orbit coupling

Hui Hu<sup>1</sup>, Lei Jiang<sup>2</sup>, Xia-Ji Liu<sup>1</sup>, and Han Pu<sup>2</sup>

<sup>1</sup>*ARC Centre of Excellence for Quantum-Atom Optics,*

*Centre for Atom Optics and Ultrafast Spectroscopy,*

*Swinburne University of Technology, Melbourne 3122, Australia*

<sup>2</sup>*Department of Physics and Astronomy, and Rice Quantum Institute, Rice University, Houston, TX 77251, USA*

Motivated by the prospect of realizing a Fermi gas with a synthetic non-Abelian gauge field, we investigate theoretically a strongly interacting Fermi gas in the presence of a Rashba spin-orbit coupling. As the two-fold spin degeneracy is lifted by spin-orbit interaction, bound pairs with mixed singlet and triplet components emerge, leading to an anisotropic superfluid. We calculate the relevant physical quantities, such as the momentum distribution, the single-particle spectral function and the spin structure factor, that characterize the system.

PACS numbers: 05.30.Fk, 03.75.Hh, 03.75.Ss, 67.85.-d

Owing to the unprecedented experimental controllability, ultracold atoms have been proven to be an ideal table-top system to study certain long-sought, challenging many-body problems. A well-known example is the crossover from a Bose-Einstein condensation (BEC) to a Bardeen-Cooper-Schrieffer (BCS) superfluid in an ultracold atomic Fermi gas [1]. Here we study a strongly interacting Fermi gas in the presence of a synthetic non-Abelian gauge field, as motivated by the recent demonstration of such field in bosonic <sup>87</sup>Rb atoms [2] and the prospect of its realization in fermionic <sup>40</sup>K atoms [3]. We focus on the Rashba spin-orbit (SO) interaction and explore its impact on the unitary Fermi gas.

It was shown in 2001 by Gor'kov and Rashba [4] that superconducting 2D metals with weak SO coupling features a mixed spin singlet-triplet pairing field, and its spin magnetic susceptibility can be dramatically affected by the SO interaction. By applying an additional large Zeeman magnetic field, it was proposed by Zhang *et al.* [5] and Sato *et al.* [6] that a topological phase with gapless edge states and non-Abelian Majorana fermionic quasiparticles may form. More recently, Vyasankere and Shenoy identified an interesting bound state by solving the two-body problem [7], referred to as *rashbons*. By increasing the strength of SO coupling, a BCS superfluid can therefore evolve into a BEC of rashbons [8].

In this Letter, we investigate the properties of Rashba SO coupled Fermi gases. We identify clearly the two-body bound state from the gaussian fluctuations of the pairing field and show that they possess anisotropic effective mass. This allows us to estimate the superfluid transition temperature in the molecular limit. We calculate various physical quantities, such as the momentum distribution, the single-particle spectral function and the spin structure factor, that are both experimentally relevant and of fundamental importance in characterizing the system. In addition, we show that the presence of the trap as in any cold atom experiment would not affect the system in any qualitative way. Therefore the salient

features of SO coupled fermions can indeed be observed in practice.

*The model* — Let us start by formulating the BEC-BCS crossover with a Rashba SO coupling  $\mathcal{H}_{so} = \lambda(\hat{k}_y \hat{\sigma}_x - \hat{k}_x \hat{\sigma}_y)$ , whose Hamiltonian is given by,

$$\mathcal{H} = \int d\mathbf{r} \left\{ \psi^\dagger [\xi_{\mathbf{k}} + \mathcal{H}_{so}] \psi + U_0 \psi_\uparrow^\dagger \psi_\downarrow^\dagger \psi_\downarrow \psi_\uparrow \right\}, \quad (1)$$

where  $\xi_{\mathbf{k}} = \hbar^2 k^2 / (2m) - \mu$ , and  $\psi(\mathbf{r}) = [\psi_\uparrow(\mathbf{r}), \psi_\downarrow(\mathbf{r})]^T$  denotes collectively the fermionic field operators. The contact *s*-wave interaction ( $U_0 < 0$ ) occurs between un-like spins. Here we give a brief description of the theoretical technique we used, the functional path integral method [9]. A more detailed account will be presented elsewhere [10]. We start from the partition function  $\mathcal{Z} = \int \mathcal{D}[\psi, \bar{\psi}] \exp \{ -S[\psi(\mathbf{r}, \tau), \bar{\psi}(\mathbf{r}, \tau)] \}$ , where  $S[\psi, \bar{\psi}] = \int_0^\beta d\tau [\int d\mathbf{r} \sum_\sigma \bar{\psi}_\sigma(\mathbf{r}) \partial_\tau \psi_\sigma(\mathbf{r}) + \mathcal{H}(\psi, \bar{\psi})]$ ,  $\beta = 1/(k_B T)$ , and  $\mathcal{H}(\psi, \bar{\psi})$  is obtained by replacing the field operators  $\psi^\dagger$  and  $\psi$  with the Grassmann variables  $\bar{\psi}$  and  $\psi$ , respectively. The interaction term can be decoupled by using the standard Hubbard-Stratonovich transformation with the introduction of a pairing field  $\Delta(\mathbf{r}, \tau)$ . After integrating out the fermionic fields, we have  $\mathcal{Z} = \int \mathcal{D}[\Delta, \bar{\Delta}] \exp \{ -S_{eff}[\Delta, \bar{\Delta}] \}$ , where  $S_{eff} = \int_0^\beta d\tau \int d\mathbf{r} \left\{ -\frac{|\Delta(\mathbf{r}, \tau)|^2}{U_0} \right\} - \frac{1}{2} \text{Tr} \ln [-\mathcal{G}^{-1}] + \beta \sum_{\mathbf{k}} \xi_{\mathbf{k}}$ , with  $\mathcal{G}$  being the single-particle Green function. To proceed, we restrict ourselves to the gaussian fluctuation and expand  $\Delta(\mathbf{r}, \tau) = \Delta_0 + \delta\Delta(\mathbf{r}, \tau)$ . The effective action is then decomposed accordingly  $S_{eff} = S_0 + \Delta S$ , where, in the momentum space, the fluctuation action takes the form  $[k \equiv (\mathbf{k}, i\omega_m)]$  and  $q \equiv (\mathbf{q}, i\nu_n)$ :  $\Delta S = \sum_{\mathbf{q}, i\nu_n} \left[ -\frac{1}{U_0} \delta\Delta(q) \delta\bar{\Delta}(q) \right] + \frac{1}{2} \left( \frac{1}{2} \right) \text{Tr}_\sigma \sum_{k, q} [\mathcal{G}_0(k) \Sigma(q) \mathcal{G}_0(k-q) \Sigma(-q)]$ , with

$$\Sigma(q) = \begin{bmatrix} 0 & i\delta\Delta(q) \hat{\sigma}_y \\ -i\delta\bar{\Delta}(-q) \hat{\sigma}_y & 0 \end{bmatrix}. \quad (2)$$

*Two-body bound state* — Let us consider first the

normal state with  $\Delta_0 = 0$ , in which case the Green function reduces to its non-interacting form as  $\mathcal{G}_0(k) = \text{Diag}\{\hat{g}_0(k), -\hat{g}_0(-k)\}$  with  $\hat{g}_0(k) = [i\omega_m - \xi_{\mathbf{k}} - \lambda(k_y\hat{\sigma}_x - k_x\hat{\sigma}_y)]^{-1}$ , leading to *two* helicity branches in the single-particle spectrum,  $E_{\mathbf{k},\alpha} = \xi_{\mathbf{k}} + \alpha\lambda k_{\perp}$ , where  $k_{\perp} \equiv (k_x^2 + k_y^2)^{1/2}$  and  $\alpha = \pm 1$ . The fluctuation action is given by  $\Delta S = \sum_{\mathbf{q}} [-\Gamma^{-1}(\mathbf{q})] \delta\Delta(\mathbf{q})\delta\bar{\Delta}(\mathbf{q})$ , where  $\Gamma^{-1}(\mathbf{q})$  is the inverse vertex function which, at  $\mathbf{q} = \mathbf{0}$ , takes the form

$$\Gamma^{-1}(\omega) = \frac{m}{4\pi\hbar^2 a_s} - \frac{1}{V} \sum_{\mathbf{k}} \left[ \sum_{\alpha=\pm} \frac{1/2 - f(E_{\mathbf{k},\alpha})}{\omega + i0^+ - 2E_{\mathbf{k},\alpha}} + \frac{1}{2\epsilon_{\mathbf{k}}} \right],$$

where  $f(x) = 1/(e^{x/k_B T} + 1)$  is the Fermi distribution function and we have renormalized the bare interaction  $U_0$  by the *s*-wave scattering length,  $1/U_0 = m/(4\pi\hbar^2 a_s) - V^{-1} \sum_{\mathbf{k}} 1/(2\epsilon_{\mathbf{k}})$ , with  $V$  being the quantization volume.

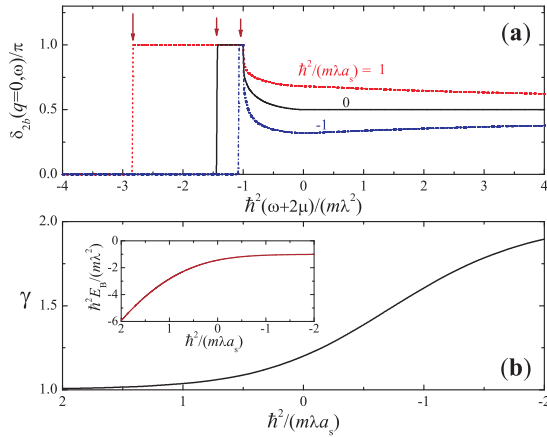


Figure 1: (Color online) (a) Rashbons as evidenced by the two-body phase shift of  $\Gamma^{-1}(\mathbf{0}, \omega)$  at three different scattering lengths. The arrows indicate the position of binding energy. (b) Effective mass of rashbons [ $\gamma = M_{\perp}/(2m)$ ] in the strong SO limit. The inset shows the bound state energy as a function of the scattering length.

The vertex function is simply the Green function of the fermion pair. A bound state can therefore be examined clearly by calculating the phase shift [11]  $\delta(\mathbf{q}, \omega) = -\text{Im} \ln[-\Gamma^{-1}(\mathbf{q}, i\nu_n \rightarrow \omega + i0^+)]$ . For a true boson, the phase shift is given by  $\delta_B(\mathbf{q}, \omega) = \pi\Theta(\omega - \epsilon_{\mathbf{q}}^B + \mu_B)$ , where  $\epsilon_{\mathbf{q}}^B$  and  $\mu_B$  are the bosonic dispersion and chemical potential, respectively, and  $\Theta(x)$  is the step function. In Fig. 1(a), we plot the two-body part of the phase shift at  $\mathbf{q} = \mathbf{0}$ , obtained by discarding Fermi functions. The phase shift jumps from 0 to  $\pi$  at a critical frequency, signaling the occurrence of a bound state. By recalling that the bosonic chemical potential is given by  $\mu_B = 2\mu - E_B$ , where  $E_B$  is the bound state energy, the critical frequency  $(\omega + 2\mu)_c$  at  $\mathbf{q} = \mathbf{0}$  gives exactly  $E_B$ . Using the fact that the critical frequency corresponds to the position where  $\text{Re}[\Gamma^{-1}]$  changes sign, we have

$$\frac{m}{4\pi\hbar^2 a_s} - \frac{1}{2V} \sum_{\mathbf{k}; \alpha=\pm} \left[ \frac{1}{E_B - 2E_{\mathbf{k},\alpha}} + \frac{1}{\epsilon_{\mathbf{k}}} \right] = 0. \quad (3)$$

The inset in Fig. 1(b) shows the bound state energy as a function of the SO coupling strength. At the unitarity limit, the bound state energy is universally given by  $E_B \approx -1.439229m\lambda^2/\hbar^2$ . The size of the bound state  $a$  is therefore at the order of  $\hbar^2/(m\lambda)$ . The bound states are only well defined once  $a \ll k_F^{-1}$  or  $\lambda k_F \gg \epsilon_F$ . Thus, we anticipate that the system will cross over to a gas of rashbons at  $\lambda k_F/\epsilon_F \sim 1$ .

In the limit of a large SO coupling, the well-defined two-body bound state should have a bosonic dispersion  $\epsilon_{\mathbf{q}}^B = \hbar^2 q_{\perp}^2/(2M_{\perp}) + \hbar^2 q_z^2/(2M_z)$  and weakly interact with each other *repulsively*. Because of the anisotropic fermionic dispersion  $E_{\mathbf{k},\pm} = \xi_{\mathbf{k}} \pm \lambda k_{\perp}$ , the effective mass of rashbons becomes anisotropic. While  $M_z = 2m$  is not affected by the Rashba coupling,  $M_{\perp}$  may get strongly renormalized. As the jump of the phase shift at nonzero  $\mathbf{q}$  which occurs at  $E_B + \epsilon_{\mathbf{q}}^B$ , we can numerically determine  $M_{\perp}$ . Fig. 1(b) displays  $\gamma = M_{\perp}/(2m)$ . At unitarity, we find  $\gamma \simeq 1.2$ . When the system becomes an ensemble of weakly interacting rashbons, the heavy mass  $M_{\perp}$  causes a decrease in the condensation temperature so that  $T_{\text{BEC}} = \gamma^{-2/3} T_{\text{BEC},0}$ , where  $T_{\text{BEC},0} \simeq 0.218 T_F$  is the BEC temperature without the SO coupling.

*Condensation of rashbons* — Let us now turn to the condensed phase characterized by a nonzero order parameter  $\Delta_0 \neq 0$ . At the mean-field saddle-point level, the single-particle Green function takes the form,

$$\mathcal{G}_0^{-1} = \begin{bmatrix} i\omega_m - \xi_{\mathbf{k}} - \mathcal{H}_{so} & i\Delta_0 \hat{\sigma}_y \\ -i\Delta_0 \hat{\sigma}_y & i\omega_m + \xi_{\mathbf{k}} - \mathcal{H}_{so}^* \end{bmatrix}. \quad (4)$$

The inversion of the above matrix can be worked out explicitly, leading to *two* single-particle Bogoliubov dispersions whose degeneracy is lifted by the SO interaction,  $E_{\mathbf{k},\pm} = \sqrt{(\xi_{\mathbf{k}} \pm \lambda k_{\perp})^2 + \Delta_0^2}$ , and the normal and anomalous Green functions from which we can immediately obtain the momentum distribution  $n(\mathbf{k}) = 1 - \sum_{\alpha} [1/2 - f(E_{\mathbf{k},\alpha})] \gamma_{\mathbf{k},\alpha}$  and the single-particle spectral function  $A_{\uparrow}(\mathbf{k}, \omega) = A_{\downarrow}(\mathbf{k}, \omega) = \sum_{\alpha} [(1 + \gamma_{\mathbf{k},\alpha}) \delta(\omega - E_{\mathbf{k},\alpha}) + (1 - \gamma_{\mathbf{k},\alpha}) \delta(\omega + E_{\mathbf{k},\alpha})] / 4$ , where  $\gamma_{\mathbf{k},\pm} = (\xi_{\mathbf{k}} \pm \lambda k_{\perp}) / E_{\mathbf{k},\pm}$ . The chemical potential and the order parameter are to be determined by the number and the gap equations,  $n = \sum_{\mathbf{k}} n(\mathbf{k})$  and  $\Delta_0 = -U_0 \Delta_0 \sum_{\alpha} [1/2 - f(E_{\mathbf{k},\alpha})] / (2E_{\mathbf{k},\alpha})$ , respectively. Fig. 2(a) displays the chemical potential  $\mu$  and order parameter as functions of the SO coupling strength for a unitary Fermi gas. The increase of the SO strength leads to a deeper bound state. As a consequence, in analogy with the BEC-BCS crossover, the order parameter and critical transition temperature are greatly enhanced at  $\lambda k_F \sim \epsilon_F$ . In the large SO coupling limit, we have  $\mu = (\mu_B + E_B)/2$ , where  $\mu_B$  is positive due to the repulsion between rashbons and decreases with increasing coupling as shown in the inset of Fig. 2(a). By assuming an *s*-wave repulsion with scattering length  $a_B$ , where  $\mu_B \simeq (n/2)4\pi\hbar^2 a_B/M$ , we estimate within

mean-field that in the unitarity limit,  $a_B \simeq 3\hbar^2/(m\lambda)$ , comparable to the size of rashbons.

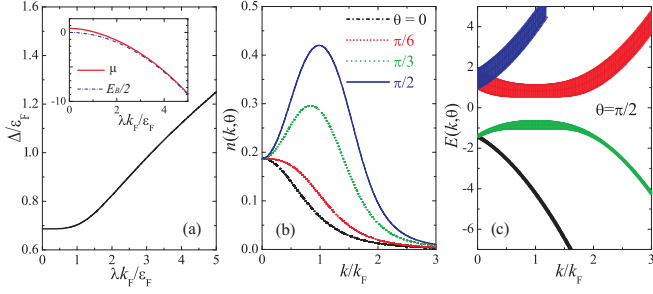


Figure 2: (a) Mean-field order parameter as a function of the SO coupling for a homogeneous unitary Fermi gas at zero temperature. The inset shows the chemical potential and the half of bound state energy, both in units of  $\epsilon_F$ . (b) Momentum distribution and (c) single-particle spectral function for  $\theta = \pi/2$  at  $\lambda k_F/\epsilon_F = 2$ . Here  $\theta$  is the angle between  $\mathbf{k}$  and the  $z$ -axis. The width of the curves in (c) represents the weight factor  $(1 \pm \gamma_{\mathbf{k}, \pm})/4$  for each of the four Bogoliubov excitations.

Figure 2(b) and (c) illustrate the momentum distribution and the single-particle spectral function, respectively. These quantities exhibit anisotropic distribution in momentum space due to the SO coupling and can be readily measured in experiment.

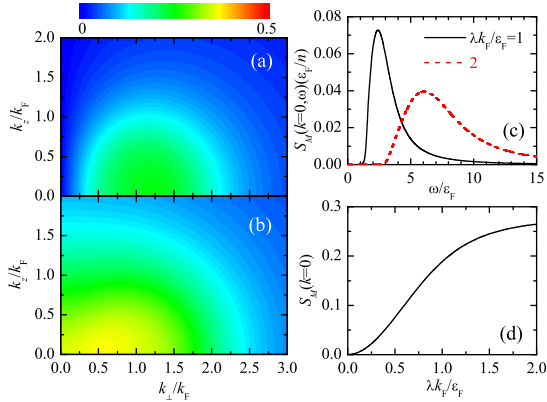


Figure 3: (Color online) Linear contour plot for the triplet pairing correlation  $|\langle \psi_{\mathbf{k}\uparrow} \psi_{-\mathbf{k}\uparrow} \rangle|$  between like spins (a) and the singlet pairing correlation  $|\langle \psi_{\mathbf{k}\uparrow} \psi_{-\mathbf{k}\downarrow} \rangle|$  between un-like spins (b) for a homogeneous unitary Fermi gas at zero temperature with  $\lambda k_F/\epsilon_F = 2$ . The zero-momentum dynamic and static spin structure factor are shown in (c) and (d), respectively.

Another important consequence of the SO coupling is that the pairing field contains both a singlet and a triplet component [4, 8]. For the system under study, it is straightforward to show that the triplet and singlet pairing fields are given by  $\langle \psi_{\mathbf{k}\uparrow} \psi_{-\mathbf{k}\uparrow} \rangle = -i\Delta_0 e^{-i\varphi_{\mathbf{k}}} \sum_{\alpha} \alpha [1/2 - f(E_{\mathbf{k},\alpha})]/(2E_{\mathbf{k},\alpha})$  and  $\langle \psi_{\mathbf{k}\uparrow} \psi_{-\mathbf{k}\downarrow} \rangle = \Delta_0 \sum_{\alpha} \alpha [1/2 - f(E_{\mathbf{k},\alpha})]/(2E_{\mathbf{k},\alpha})$ , respectively, where  $e^{-i\varphi_{\mathbf{k}}} \equiv (k_x - ik_y)/k_{\perp}$ . The magnitude of the pairing fields are shown in Fig. 3(a) and (b).

The weight of the triplet component increases and approaches that of the singlet component as the SO coupling strength increases. In Fig. 3(c) and (d), we plot the zero-momentum dynamic and static spin structure factor [12], respectively. In the absence of the SO coupling, both these quantities vanish identically. Hence a nonzero spin structure factor is a direct consequence of triplet pairing [4]. Note that spin structure factor can be measured using the Bragg spectroscopy method as demonstrated in recent experiments [13].

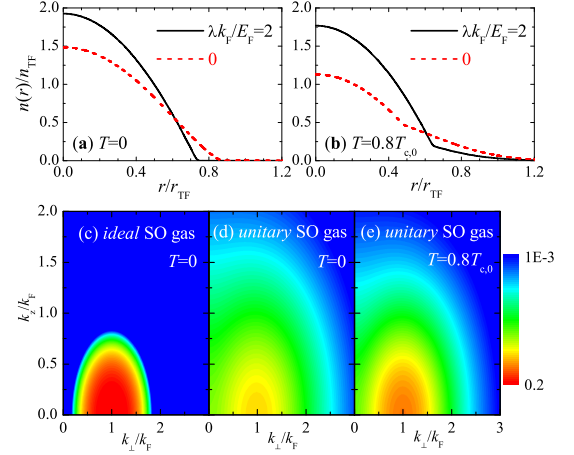


Figure 4: (Color online) Density distributions of a trapped unitary Fermi gas at  $T = 0$  (a) and  $T = 0.8T_{c,0}$  (b).  $T_{c,0}$  is the critical temperature in the absence of the SO coupling. (c), (d) and (e) display the log-scale contour plot of the momentum distribution for a trapped SO coupled ideal gas at  $T = 0$ , unitary gas at  $T = 0$  and unitary gas at  $T = 0.8T_{c,0}$ , respectively. Here the Fermi energy is given by  $E_F = (3N)^{1/3}\hbar\omega_0$ , Fermi wave number  $k_F = (24N)^{1/6}a_{ho}^{-1}$ , Thomas-Fermi radius  $r_{TF} = (24N)^{1/6}a_{ho}$ , and the non-interacting peak density  $n_{TF} = (24N)^{1/2}/(3\pi^2)a_{ho}^{-3}$ , where  $a_{ho} = \sqrt{\hbar/(m\omega)}$  is the characteristic length of the harmonic oscillator.

*Probing the anisotropic superfluid* — One leading candidate to observe superfluid rashbons is a trapped Fermi gas of  $^{40}\text{K}$  atoms near a broad Feshbach resonance, where an applicable scheme to generate the Rashba SO coupling was recently proposed [3]. Previous experiments have demonstrated the measurement of momentum distribution and single-particle spectral function in  $^{40}\text{K}$  without the SO coupling [14]. We perform the mean-field calculation in a 3D spherical harmonic trap  $V_T(r) = m\omega_0^2 r^2/2$ , by using the local density approximation (LDA) [15]. In LDA, the gas is divided into small cells with a local chemical potential  $\mu(r) = \mu_0 - V_T(r)$ , where  $\mu_0$  can be determined by the number equation  $\int dr n(r) = N$ , where  $N$  is the total number of fermions. The local density  $n(r)$ , momentum distribution  $n(\mathbf{k}; r)/(2\pi)^3$ , occupied spectral function  $A(\mathbf{k}, \omega; r)f(\omega)k^2/(2\pi^2)$  are then integrated over the whole space to obtain the total contribution. We show, in Fig. 4(a) and (b), the density profiles of a trapped unitary Fermi gas at different SO coupling

strengths and temperatures. As anticipated, with the increase of the SO coupling the cloud shrinks. As shown in Fig. 4(c)-(e), the anisotropic momentum distribution at large SO coupling, which can be measured using the time-of-flight technique, is not washed out by the trap. This anisotropy originates from the SO coupling, which also manifests itself in a non-interacting system [see Fig. 4(c)]. However, by comparing Fig. 4(c) with (d) and (e), one can clearly see the effects of the interaction which greatly widens the momentum distribution.

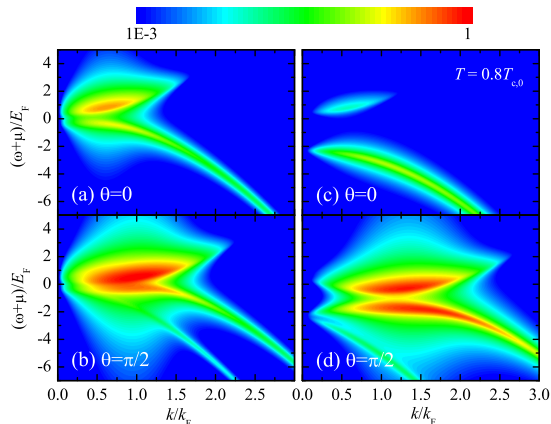


Figure 5: (Color online) Log-scale contour plot of the single-particle spectral function for a trapped unitary Fermi gas at  $T = 0.8T_{c,0}$ . The SO coupling strength in (a) and (b) is  $\lambda k_F/E_F = 1$ , and in (c) and (d) is  $\lambda k_F/E_F = 2$ .

Figure 5 presents the occupied spectral function at  $T = 0.8T_{c,0}$ , where  $T_{c,0}$  is the critical temperature without the SO interaction. The distinct behavior for the spectral function at  $\theta = 0$  (along the  $z$ -axis) and  $\pi/2$  (in the transverse plane) can be probed by the recently demonstrated momentum-resolved rf-spectroscopy [14]. To make better comparison with the experiment, we have included in the calculation an energy resolution of  $0.2E_F$ , as presented in the JILA rf-measurement. Both Fig. 4 and Fig. 5 therefore clearly demonstrate that the anisotropic nature of the rashbon superfluid will not be smeared out by averaging over the trapped cloud.

**Summary** — We have shown that Fermi superfluid subject to a strong Rashba spin-orbit coupling differ significantly from the conventional BEC-BCS crossover system studied intensively over the past few years. Rashbons — the two-body bound states induced by the SO coupling — have anisotropic effective mass and condense into a mixed spin pairing state. They lead to a strong anisotropy in the momentum distribution and the single-particle spectral function as well as a higher critical temperature. We have proposed that these distinct behaviors can be readily probed in a trapped strongly interacting Fermi gas of  $^{40}\text{K}$  atoms in a synthetic non-Abelian gauge field.

More interesting properties of the system may be dis-

covered thanks to the unprecedented controllability in ultracold atoms. SO coupled Fermi gas in 2D may be utilized to create Majorana fermions [5, 16]. Topological phase transitions may be induced by an additional Zeeman field [16]. Therefore, the exploration of strong correlation effects of SO coupled Fermi gases represents a new exciting avenue of research in many-body problem. In the current work, we have adopted a mean-field approach. The mean-field calculation in the condensed phase can be improved by incorporating gaussian pair fluctuations [17] in the future.

**Acknowledgment** — HH and XJL was supported by the ARC Discovery Projects No. DP0984522 and No. DP0984637. HP is supported by the NSF and the Welch Foundation (C-1669). We thank Chuanwei Zhang, Hui Zhai and Shizhong Zhang for many useful discussions.

**Note added:** After completing our work, we noticed the work of Ref. [18] which treats a similar system. Our results agree with each other where they overlap.

- 
- [1] S. Giorgini, L. P. Pitaevskii, and S. Stringari, *Rev. Mod. Phys.* **80**, 1215 (2008).
  - [2] Y.-J. Lin *et al.*, *Phys. Rev. Lett.* **102**, 130401 (2009); Y.-J. Lin, K. Jimenez-Garcia, and I. B. Spielman, *Nature (London)* **471**, 83 (2011).
  - [3] J. D. Sau *et al.*, *Phys. Rev. B* **83**, 140510(R) (2011).
  - [4] L. P. Gor'kov, and E. I. Rashba, *Phys. Rev. Lett.* **87**, 037004 (2001).
  - [5] C. Zhang *et al.*, *Phys. Rev. Lett.* **101**, 160401 (2008).
  - [6] M. Sato, Y. Takahashi, and S. Fujimoto, *Phys. Rev. Lett.* **103**, 020401 (2009); *Phys. Rev. B* **82**, 134521 (2010).
  - [7] J. P. Vyasanakere, and V. B. Shenoy, *Phys. Rev. B* **83**, 094515 (2011).
  - [8] J. P. Vyasanakere, S. Zhang and V. B. Shenoy, *Phys. Rev. B* **84**, 014512 (2011).
  - [9] C. A. R. Sá de Melo, Mohit Randeria, and Jan R. Engelbrecht, *Phys. Rev. Lett.* **71**, 3202 (1993).
  - [10] L. Jiang *et al.*, in preparation.
  - [11] P. Nozières and S. Schmitt-Rink, *J. Low Temp. Phys.* **59**, 195 (1985).
  - [12] R. Combescot, S. Giorgini and S. Stringari, *Europhys. Lett.* **75** 695 (2006).
  - [13] G. Veeravalli *et al.*, *Phys. Rev. Lett.* **101**, 250403 (2008); E. D. Kuhnle *et al.*, *Phys. Rev. Lett.* **105**, 070402 (2010); *Phys. Rev. Lett.* **106**, 170402 (2011).
  - [14] J.T. Stewart, J.P. Gaebler, and D.S. Jin, *Nature* **454**, 744 (2008); J.P. Gaebler *et al.*, *Nature Phys.* **6**, 569 (2010).
  - [15] A more self-consistent way of incorporating the trapping potential is to use the Bogoliubov-de Gennes (BdG) approach suitable for inhomogeneous Fermi superfluid. A BdG study of SO coupled Fermi gas is under way.
  - [16] S. Tewari *et al.*, *New J. Phys.* **13**, 065004 (2011); M. Gong, S. Tewari, and C. Zhang, arXiv:1105.1796 (2011).
  - [17] H. Hu, X.-J. Liu, and P. D. Drummond, *Europhys. Lett.* **74**, 574 (2006).
  - [18] Z.-Q. Yu, and H. Zhai, arXiv:1105.2250 (2011).